DALTON
FULL PAPER

Stereospecific assembly of chiral Λ-Cr(III)-Δ-Ln(III)-oxalato-bridged dinuclear 3d–4f complexes (Ln = Yb or Dy) and near infrared circular dichroism in the 4f→4f transitions

Md. Abdus Subhan, Takayoshi Suzuki and Sumio Kaizaki *

Department of Chemistry, Graduate School of Science, Osaka University, Toyonaka, Osaka, 560-0043, Japan. E-mail: kaizaki@chem.sci.osaka-u.ac.jp

Received 12th September 2000, Accepted 21st December 2000
First published as an Advance Article on the web 30th January 2001

Stereospecific formation of the chiral heterodinuclear 3d–4f complexes (Λ–Δ)-[$(acac)_2Cr(ox)Ln(HBpz_3)_2$] ($acac^-$ = acetylacetonate, ox^{2-} = oxalato, $HBpz_3^-$ = hydrotris(pyrazol-1-yl)borato; Ln = Yb: **1**, Dy: **2** where (Λ–Δ) implies the absolute configuration around the octahedral Cr and square antiprismatic Ln moiety, respectively) was demonstrated by comparing the near infrared circular dichroism (NIR CD) in the 4f→4f transitions and/or the single crystal X-ray analysis with those of a diastereomeric mixture of the mononuclear Λ-, and Δ-[$Yb(HBpz_3)_2$(*S*-pba)] **3** (*S*-pba = *S*-(+)-2-phenylbutyrate) complex. The NIR CD spectra for the 4f→4f transitions of the 3d–4f (Λ–Δ)-Cr(ox)Ln complexes **1** and **2** with configurational chirality around the Ln ion with no asymmetric carbon were observed for the first time in CH_2Cl_2.This observation is supported by the selection rule for the optical activity of the 4f→4f transitions. The first solution NIR magnetic circular dichroism (MCD) of the racemic Cr(ox)Yb and Cr(ox)Dy complexes is also reported.

Introduction

Chiroptical properties as well as the stereochemistry of chiral lanthanide(III) complexes provide valuable information on biological systems. To date, in spite of the importance of chirality and dimensionality in Ln complexes as biological probes and/or precursors for supramolecules,[1,2] there have been only a limited number of systematic investigations on the optical activity of structurally rigid lanthanide complexes. This drawback may be due to the limited number of stable configurationally chiral Ln complexes, a direct consequence of the synthetic difficulty associated with the lability of lanthanide complexes. Some solution circular dichroism (CD) spectra of Ln(III) complexes with L-α-amino carboxylate and other chiral ligands have been reported.[3–5]

For Eu(III) and Tb(III) complexes with chiral β-diketonate derived from d-camphor as well as optically active aminopolycarboxylate or 1,4,7,10-tetraazacyclododecane derivatives, which could induce configurational chirality, chiroptical spectra (circularly polarized luminescence (CPL)[6] or CD[7–9]) have offered excellent opportunities for the examination of the optical activity theory as well as the chiroptical–structural relation in chiral Ln(III) systems. Very recently, CD spectra of Yb(III) complexes with optically active DOTMA (1*R*,4*R*,7*R*,10*R*-α,α′,α″,α‴-tetramethyl-1,4,7,10-tetraazacyclododecane-1,4,7,10-tetraacetate) and related ligands were reported for the first time,[10] following CPL studies.[11–13] In parallel, the NMR spectroscopy of Ln complexes with the analogous ligands has been used for chiral recognition.[14] However, much attention could be paid to chiroptical spectroscopy of configurationally chiral Yb(III) complexes with other types of ligands. One of the candidates for the formation of configurationally chiral lanthanide complexes would be a hydrotris(pyrazol-1-yl)borato ($HBpz_3^-$), a tridentate tripodal type ligand; due to its expected reluctance to undergo racemization as assumed from the fact that the eight-coordinate [$Yb(HBpz_3)_3$] complex was found to be rigid in solution by NMR spectroscopy.[15]

Recently, we reported the synthesis, structures and/or magneto-optical properties in a series of novel tri- and dinuclear complexes, [$Ni(L)\{Ln(HBpz_3)_2\}_2$] (L = 1,3-trimethylenebis(oxamidate) and 1,2-ethylenebis(oxamidate)) with a linear Ln(III)–Ni(II)–Ln(III) structure[16] and [$Cr(acac)_2(ox)Ln(HBpz_3)_2$] (where Ln = Eu, Gd, Tb, Yb, Lu and $acac^-$ = acetylacetonato, ox^{2-} = oxalato).[17] The single crystal X-ray structural analysis of **1**[17] demonstrated a six coordinate octahedral *OC*-6-Cr and an eight coordinate square antiprismatic, *SAPR*-8-Ln configuration. There are two molecules with Λ_{OC}–Δ_{SAPR} and Δ_{OC}–Λ_{SAPR} absolute configurations in the unit cell. For this result, there were considered to be two possibilities of either a stereospecific formation or an accidental pickup of the racemic mixture.[17]

The present work aims to determine the chiral assembly between Λ-[$Cr(acac)_2(ox)]^-$ and Δ-[$Ln(HBpz_3)_2]^+$ resulting in the formation of the chiral (Λ–Δ)-Cr(ox)Ln complexes, (Λ–Δ)-[$(acac)_2Cr(ox)Ln(HBpz_3)_2$] (Ln = Yb **1** and Dy **2**) on the basis of single crystal X-ray structural analysis and CD spectra in comparison with those of the related mononuclear [$Yb(HBpz_3)_2$(*S*-pba)] **3**.

Experimental

Materials

All chemicals were of reagent grade and were used without further purification. The ligand potassium hydrotris(pyrazol-1-yl)borate was prepared by a similar method to that described by Trofimenko.[18]

Optical resolution of $Na[Cr(acac)_2(ox)]\cdot H_2O$

This was performed by a modified method analogous to that for the corresponding Co(III) complex.[19] After a mixture of the resolving agent (−)†-*cis*-$[Co(NO_2)_2(en)_2]Br$ (0.46 g, 1.3×10^{-3} mol) and $AgCH_3COO$ (0.22 g, 1.3×10^{-3} mol) was suspended in 2 ml of H_2O with vigorous shaking for 10 min, the precipitate (AgBr) was filtered and washed with water. To a combined solution of this filtrate and washings was added Na[Cr-

† Note hereafter that the signs of the optical rotation prefixed to the chemical formula, (+) or (−), are those of the major CD component in the first spin-allowed band region.

 DOI: 10.1039/b007369p

$(acac)_2(ox)]\cdot H_2O$ (1 g, 2.6×10^{-3} mol) with stirring. A pale green product was precipitated. The precipitate was collected on a glass filter and washed with methanol and acetone several times. Two more fractions of the pale green product were obtained from the filtrate by concentration. The pale green diastereomer (+)-[$Cr(acac)_2(ox)$]·(−)-*cis*-[$Co(NO_2)_2(en)_2$] was recrystallized from a minimum amount of water. An aqueous solution of the diastereomer was passed through an SP-Sephadex C-25(Na^+) column. The purple band was collected by eluting with water, leaving the yellow band of the resolving agent, (−)-*cis*-$[Co(NO_2)_2(en)_2]^+$ on top of the column. After the eluate was concentrated to dryness on a rotary evaporator, a purple powder was collected. Anal. Calc. for $C_{12}H_{17}O_{9.5}CrNa$((+)-Na[$Cr(acac)_2(ox)$]·$1.5H_2O$): C, 37.12%; H, 4.41%. Found: C, 37.11%; H, 4.37%. $\Delta\varepsilon_{ext} = +3.75$ dm^3 mol^{-1} cm^{-1} at 532 nm in methanol.

The purple filtrate obtained after the separation of the pale green diastereomer ((+)-[$Cr(acac)_2(ox)$]·(−)-*cis*-[$Co(NO_2)_2(en)_2$]) was evaporated to dryness and then treated with (+)-*cis*-$[Co(NO_2)_2(en)_2]Br$ to obtain the diastereomer (−)-[$Cr(acac)_2(ox)$]·(+)-*cis*-$[Co(NO_2)_2(en)_2]$. The enantiomer (−)-Na[$Cr(acac)_2(ox)$]·$1.5H_2O$ was then obtained by the same procedure as for (+)-Na[$Cr(acac)_2(ox)$]·$1.5H_2O$. Anal. Calc. for $C_{12}H_{17}O_{9.5}CrNa$((−)-Na[$Cr(acac)_2(ox)$]·$1.5H_2O$): C, 37.12%; H, 4.41%. Found: C, 37.13%; H, 4.27%. $\Delta\varepsilon_{ext} = -3.75$ dm^3 mol^{-1} cm^{-1} at 532 nm in methanol.

Since the absolute value of the CD intensities for both the enantiomers was identical this optical resolution was found to be complete.

Preparation of (Λ–Δ)-[$(acac)_2Cr(ox)Ln(HBpz_3)_2$]·$n CH_2Cl_2$

The Yb and Dy complexes were prepared from (+)-Na[$Cr(acac)_2(ox)$]·$1.5H_2O$ by the same aqueous method as for the racemic complexes[17] and also by the newly developed non-aqueous method. The latter, new method, gave a slightly improved yield compared to the previous one as follows. $Ln(CF_3SO_3)_3$ (0.2 mmol) in 15 cm^3 of THF was stirred in a beaker for 5 min. After this time $KHBpz_3$ (0.1 g, 0.4 mmol) in 10 cm^3 of THF and (+)-Na[$Cr(acac)_2(ox)$]·$1.5H_2O$ (0.078 g, 0.2 mmol) in 10 cm^3 of MeOH were added to the solution and stirring was continued for a further 10 min. A clear purple-red solution was obtained. The reaction mixture was kept in a refrigerator overnight. After filtration to remove any insoluble material, the mixture was evaporated to dryness and then dried *in vacuo*. The crude product was crystallized from CH_2Cl_2–hexane solution. The tablet product obtained was purified by a recycling preparative HPLC (LC-908, Japan Analytical Industry Co. Ltd.) using $CHCl_3$ as eluant. The second band was collected and crystallization was performed from $CHCl_3$–hexane solution. The recrystallizations were carried out several times by slowly evaporating the complex solution in a mixture of dichloromethane and hexane. The yields were 30% for the Yb complex and 15% for the Dy complex. Anal. Calc. for $C_{32}H_{38}B_2Cl_4CrN_{12}O_8Yb$ (**1**·$2CH_2Cl_2$): C, 34.71%; H, 3.46%; N, 15.18%; Found: C, 35.02%; H, 3.43%; N, 15.40%.

Anal. Calc. for $C_{31}H_{36}B_2Cl_2CrN_{12}O_8Dy$ (**2**·CH_2Cl_2): C, 36.80%; H, 3.59%; N, 16.61%; Found: C, 37.40%; H, 3.71%; N, 16.81%.

Positive FAB mass for the Dy complex: *m*/*z* 927($[M + H]^+$, 5.6%), *m*/*z* 827($[M - acac]^+$, 20%), *m*/*z* 589 ($[Dy(HBpz_3)_2]^+$, 100%) where $M = 926$ for (Λ–Δ)-[$(acac)_2Cr(ox)Dy(HBpz_3)_2$].

Preparation of [$Yb(HBpz_3)_2$(*S*-pba)] 3

Complex **3** was prepared by a similar method to that for the corresponding acetate complex.[20] The crude product was recrystallized from a mixture of dichloromethane–hexane to deposit single crystals suitable for X-ray analysis. The yield was 60%. The corresponding [$Yb(HBpz_3)_2$(*RS*-pba)] **4** was obtained by the same method as for the *S*-pba complex, **3**. Anal. Calc. for $C_{28}H_{31}C_2N_{12}O_2Yb$ (**3** and **4**): C, 44.12%; H, 4.10%; N, 22.05%; Found for [$Yb(HBpz_3)_2$(*S*-pba)]: C, 44.41%; H, 4.07%; N, 21.72%; Found for [$Yb(HBpz_3)_2$(*RS*-pba)]: C, 44.61%; H, 4.21%; N, 20.98%.

Measurements

Absorption spectra were measured on a Perkin-Elmer Lambda-19 spectrophotometer. CD data were collected on a Jasco J-720W spectropolarimeter. MCD spectra were recorded on a Jasco J-720W spectropolarimeter in a magnetic field of 1.5 T (1 T = 10,000 Gauss) at room temperature.

Crystal structure determination

A purple polyhedral crystal of the complex **1**·$2CH_2Cl_2$ and a colorless columnar crystal of complex **3** were sealed in a glass capillary tube to prevent possible efflorescence. The X-ray intensities ($2\theta_{max} = 60°$) were measured on a Rigaku AFC-5R, and absorption corrections were made by either the empirical Ψ-scan method[21] or the numerical integration method.[22] The structures were solved by the direct method using SHELXS86 program,[23] and refined on F^2 against all reflections by the full-matrix least-squares technique using anisotropic thermal parameters for all non-hydrogen atoms. Hydrogen atoms were placed at the positions generated by theoretical calculations and fixed during the structural refinement cycles. All calculations were carried out using a TeXsan software package.[24] The details of structure analysis for each compound are given below.

Complex **1**·$2CH_2Cl_2$: systematic absences indicated the non-centrosymmetric space group $P2_12_12_1$ in the orthorhombic crystal system. The absolute structure of the complex was assumed to be the Λ-Cr(ox)Yb isomer on the basis of the starting Cr complex used. This assumption seemed to be reasonable, since the Flack's analysis[25] gave a satisfactory parameter of 0.07(3). There were severe positional disorders for the solvated dichloromethane molecules, so that all atoms of the two solvated CH_2Cl_2 molecules were fixed during structural refinement cycles at the possible positions obtained by difference-Fourier synthesis.

Complex **3**: the structure was successfully solved on the assumption of the monoclinic space group $P2_1$. Two crystallographically independent molecules, which corresponded to Δ-[$Yb(HBpz_3)_2$(*S*-pba)] and Λ-[$Yb(HBpz_3)_2$(*S*-pba)], were obtained. The absolute structures were assigned from the *S*-pba moiety, and the Flack parameter was 0.00(1).

CCDC reference number 186/2323.

See http://www.rsc.org/suppdata/dt/b0/b007369p/ for crystallographic files in .cif format.

Results and discussion

Crystallographic studies and configurational chirality

Crystallographic data for **1**·$2CH_2Cl_2$ and **3** are summarized in Table 1 and their selected bond lengths and angles (around the Yb moieties only) are given in Table 2. Their ORTEP[35] views are illustrated in Figs. 1 and 2.

The overall molecular structures around (+)-Λ-[$Cr(acac)_2(ox)]^-$ and Δ-$Yb(HBpz_3)_2^+$ in the chiral complex **1**·$2CH_2Cl_2$ are similar to those in the racemic one. The latter has a twofold symmetry axis, but **1**·$2CH_2Cl_2$ has not. The bond lengths and angles of **1**·$2CH_2Cl_2$ are somewhat different from those of the racemate,[17] as shown in Table 2. Although the absolute configuration is determined to be Λ-$[Cr(acac)_2(ox)]^-$ and Δ-$Ln(HBpz_3)_2^+$ by the single crystal X-ray analysis, it does not necessarily follow that the X-ray result is sufficient evidence for the stereospecific formation of only a diastereomeric pair ((Λ–Δ)-Cr(ox)Yb).

In contrast, the crystal structure analysis of complex **3** shows the presence of two crystallographically independent

diastereomeric molecules in the unit cell as shown in Fig. 2(a) and (b), respectively. It is noted that the bond lengths and angles of the diastereomers are different from each other within 1.6% and 3.6%, respectively, as shown in Table 2.

The reasonable geometry around the eight coordinate $Yb(N_6O_2)$ ions seems to be a square antiprismatic (*SAPR*) from the δ and φ values as summarized in Table 3. The δ_1 and δ_2 values showing planarity of the squares for the chiral complex **1**·$2CH_2Cl_2$ are 16.44° and 6.66°, respectively, whereas those values for the racemic-Cr(ox)Yb are both 8.99°.[17] Thus the chiral complex **1**·$2CH_2Cl_2$ is also on a geometric pathway to *DD* (dodecahedron) and *TPRS* (bicapped trigonal prism) as similarly for the racemic one. For both of the Δ- and Λ-[$Yb(HBpz_3)_2$(*S*-pba)] complexes, on the other hand, the geometry around the eight coordinate $Yb(N_6O_2)$ ion is not only considered to be *SAPR*, but also looks like being on a geometric pathway close to asymmetric *TPRS* with a bicapped carboxylate oxygen and $HBpz_3^-$ nitrogen. However, the differences in some δ and φ values between the diastereomers are significant, as seen in Table 3. Thus, the configurational chirality is also designated in terms of the absolute configuration *SAPR*[17] for Λ-[$Yb(HBpz_3)_2$(*S*-pba)] and Δ-[$Yb(HBpz_3)_2$-(*S*-pba)] as shown in Fig. 2(a) and (b), respectively, as adopted for the complex **1**·$2CH_2Cl_2$. For the Cr(ox)Dy complex, for which crystals suitable for X-ray analysis could not be obtained, similar configurational chirality may be examined on the basis of the CD (*vide infra*) assuming the dinuclear structure evidenced by the positive FAB mass data (see the Experimental section) found for the other racemic complexes.[17]

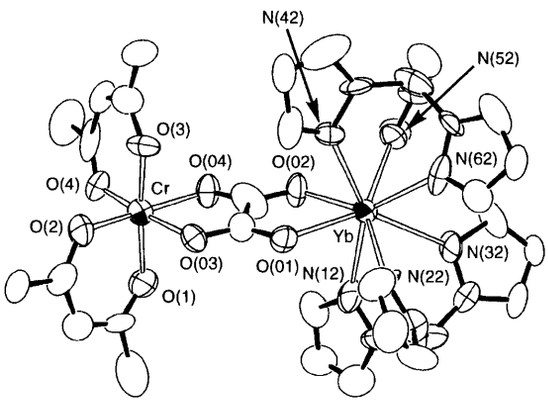

Fig. 1 ORTEP view of (Λ–Δ)-[$(acac)_2$Cr(ox)Yb$(HBpz_3)_2$] **1**.

Table 1 Crystallographic data for **1**·$2CH_2Cl_2$ and **3**

	1·$2CH_2Cl_2$	**3**
Formula	$C_{32}H_{38}B_2Cl_4CrN_{12}O_8Yb$	$C_{28}H_{31}B_2N_{12}O_2Yb$
M	1107.20	762.29
T/K	23	23
λ(Mo-Kα)/Å	0.71073	0.71073
Crystal system	Orthorhombic	Monoclinic
Space group	$P2_12_12_1$ (no. 19)	$P2_1$ (no. 4)
a/Å	15.541(4)	14.826(3)
b/Å	21.235(3)	13.344(5)
c/Å	14.199(4)	17.139(2)
β/°		105.537(8)
V/Å^3	4685(1)	3252.4(6)
Z	4	4
$\rho_{calc.}$/g cm^{-3}	1.569	1.557
μ(Mo-Kα)/cm^{-1}	25.00	29.22
$R1(F^2)$	0.077	0.028
$wR2(F^2)$	0.243	0.061

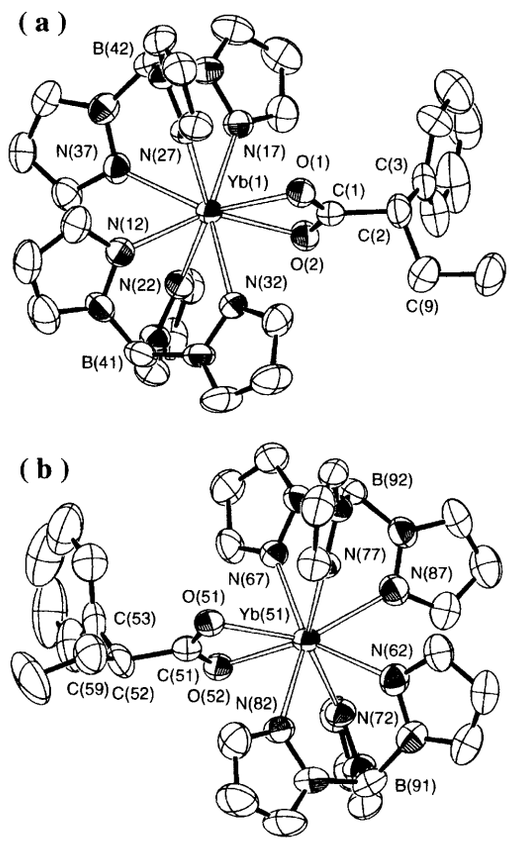

Fig. 2 ORTEP drawings of two crystallographically independent molecules of complex **3**: (a) Δ-[$Yb(HBpz_3)_2$(*S*-pba)] and (b) Λ-[$Yb(HBpz_3)_2$(*S*-pba)].

Table 2 Selected bond lengths (Å) and angles (°) for (Λ–Δ)-Cr(ox)Yb (**1**) and Δ- and Λ-[$Yb(HBpz_3)_2$(*S*-pba)] (**3**)

(Λ–Δ)-Cr(ox)Yb		Δ-[$Yb(HBpz_3)_2$(*S*-pba)]		Λ-[$Yb(HBpz_3)_2$(*S*-pba)]	
Yb–O(01)	2.34(1)	Yb(1)–O(1)	2.348(4)	Yb(51)–O(51)	2.386(4)
Yb–O(02)	2.30(1)	Yb(1)–O(2)	2.373(4)	Yb(51)–O(52)	2.342(4)
Yb–N(12)	2.52(2)	Yb(1)–N(12)	2.458(6)	Yb(51)–N(62)	2.478(5)
Yb–N(42)	2.49(2)	Yb(1)–N(17)	2.441(6)	Yb(51)–N(67)	2.473(5)
Yb–N(22)	2.47(2)	Yb(1)–N(22)	2.387(4)	Yb(51)–N(72)	2.388(5)
Yb–N(52)	2.42(2)	Yb(1)–N(27)	2.375(4)	Yb(51)–N(77)	2.376(4)
Yb–N(32)	2.49(2)	Yb(1)–N(32)	2.455(5)	Yb(51)–N(82)	2.489(6)
Yb–N(62)	2.47(2)	Yb(1)–N(37)	2.495(4)	Yb(51)–N(87)	2.470(6)
O(01)–Yb–O(02)	70.9(5)	O(1)–Yb(1)–O(2)	55.5(1)	O(51)–Yb(51)–O(52)	55.6(1)
N(12)–Yb–N(22)	76.0(8)	N(12)–Yb(1)–N(22)	80.5(2)	N(62)–Yb(51)–N(72)	77.6(2)
N(42)–Yb–N(52)	76.7(7)	N(17)–Yb(1)–N(27)	77.8(2)	N(67)–Yb(51)–N(77)	79.4(2)
N(12)–Yb–N(32)	68.5(7)	N(12)–Yb(1)–N(32)	69.2(2)	N(62)–Yb(51)–N(82)	70.1(2)
N(42)–Yb–N(62)	72.4(7)	N(17)–Yb(1)–N(37)	71.7(2)	N(67)–Yb(51)–N(87)	70.8(2)
N(22)–Yb–N(32)	78.4(7)	N(22)–Yb(1)–N(32)	77.6(2)	N(72)–Yb(51)–N(82)	79.6(2)
N(52)–Yb–N(62)	78.3(7)	N(27)–Yb(1)–N(37)	77.8(2)	N(77)–Yb(51)–N(87)	80.2(2)

Table 3 Values of δ and φ (°) for (Λ–Δ)-Cr(ox)Yb, **1** and Δ, Λ-[Yb(HBpz$_3$)$_2$(*S*-pba)], **3**[a]

(Λ–Δ)-Cr(ox)Yb		Δ-[Yb(HBpz$_3$)$_2$(*S*-pba)]		Λ-[Yb(HBpz$_3$)$_2$(*S*-pba)]	
δ_1: O(01)[N(42)N(22)]N(62)	16.44	N(37)[N(17)N(22)]O(02)	24.61	N(87)[N(67)N(72)]O(52)	21.10
δ_2: O(02)[N(12)N(52)]N(32)	6.66	N(27)[N(12)O(01)]N(32)	10.92	N(77)[N(62)O(51)]N(82)	23.12
δ_3: O(01)[N(12)N(22)]N(32)	54.72	N(27)[N(17)O(01)]O(02)	39.81	N(77)[N(67)O(51)]O(52)	47.35
δ_4: O(02)[N(42)N(52)]N(62)	56.05	N(37)[N(12)N(22)]N(32)	44.14	N(87)[N(62)N(72)]N(82)	51.51
φ_1: N(22)–O(01)–O(02)–N(52)	24.19	N(37)–N(27)–N(22)–O(01)	17.86	N(87)–N(77)–N(72)–O(51)	26.63
φ_2: N(42)–N(62)–N(32)–N(12)	19.44	O(02)–N(32)–N(17)–N(12)	10.24	O(52)–N(82)–N(67)–N(62)	18.10

[a] The notation is based on: M. G. B. Drew, *Coord. Chem. Rev.*, 1977, **24**, 179. The δ and φ values for idealized polyhedra are: *SAPR*; $\delta_1 = 0.0$, $\delta_2 = 0.0$, $\delta_3 = 52.5$, $\delta_4 = 52.5$, $\varphi_1 = 24.5$, $\varphi_2 = 24.5$, *DD*; $\delta_1 = 29.5$, $\delta_2 = 29.5$, $\delta_3 = 29.5$, $\delta_4 = 29.5$, $\varphi_1 = 0.0$, $\varphi_2 = 0.0$, *TRPS*; $\delta_1 = 21.8$, $\delta_2 = 0.0$, $\delta_3 = 48.2$, $\delta_4 = 48.2$, $\varphi_1 = 14.1$, $\varphi_2 = 14.1$.

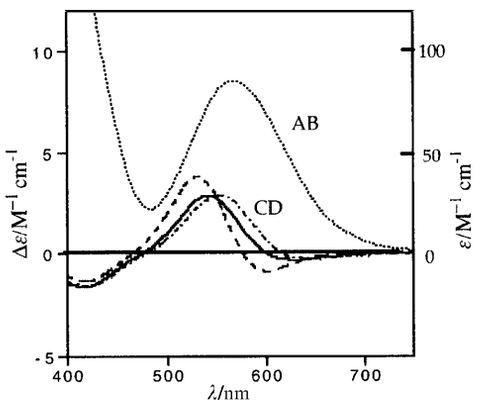

Fig. 3 Visible absorption (AB) (·····) of $[Cr(acac)_2(ox)]^-$ and circular dichroism (CD) of (+)-$[Cr(acac)_2(ox)]^-$(- - - - -) in MeOH, (Λ–Δ)-$[(acac)_2Cr(ox)Yb(HBpz_3)_2]$ (——), and (Λ–Δ)-$[(acac)_2Cr(ox)$-$Dy(HBpz_3)_2]$ (- · - · - ·) in CH_2Cl_2.

Circular dichroism in the d→d transitions

The visible absorption and CD spectra of (+)-$[Cr(acac)_2(ox)]^-$ in MeOH, **1** and **2** in CH_2Cl_2 in the d→d transitions are given in Fig. 3.

(+)-$[Cr(acac)_2(ox)]^-$ gives a positive major CD component at 532 nm in the first ligand field $^4A_2 \rightarrow {}^4T_2$ band region as shown in Fig. 3. Thus, the absolute configuration of this complex is assumed to be a Λ in terms of the empirical method based on the major CD component in the first absorption band region.[26] This assignment is also confirmed by the CD behaviour in the UV-Vis region where the ligand field and intraligand and/or charge transfer CD bands are similar in pattern and sign to those of the (+)-$[Cr(acac)_3]$ complex with an absolute configuration Λ as determined by single crystal X-ray analysis.[27] There is no observation of the CD intensity change of (+)-$[Cr(acac)_2(ox)]^-$ in methanol for several days, indicating the inertness towards racemization of the mononuclear Cr(III) complex. The complexes **1** and **2** also exhibit major positive CD components near 550 nm in the first ligand field $^4A_2 \rightarrow {}^4T_2$ d→d transition region of the Cr(III) chromophore as in Fig. 3. This fact indicates that the Λ absolute configuration around the Cr(III) ion in the (Λ–Δ)-Cr(ox)Ln complexes is retained after formation of the dinuclear entities. The CD envelopes in the (Λ–Δ)-Cr(ox)Ln complexes are somewhat altered; there is a shift to lower frequency and the signal intensity decreases due to the oxalate bridging, as also observed for the absorption spectra.[17]

Chiroptical spectra in the 4f→4f transitions

The racemic-Cr(ox)Yb and the chiral complex **1** give two groups of MCD and CD components around 975 nm (10260 cm^{-1}) and 927 nm (10790 cm^{-1}), respectively, where the corresponding absorption bands due to the $^2F_{7/2} \rightarrow {}^2F_{5/2}$ transition within the 4f^{13} electronic configuration are observed. The former group consists of negative and positive MCD peak and

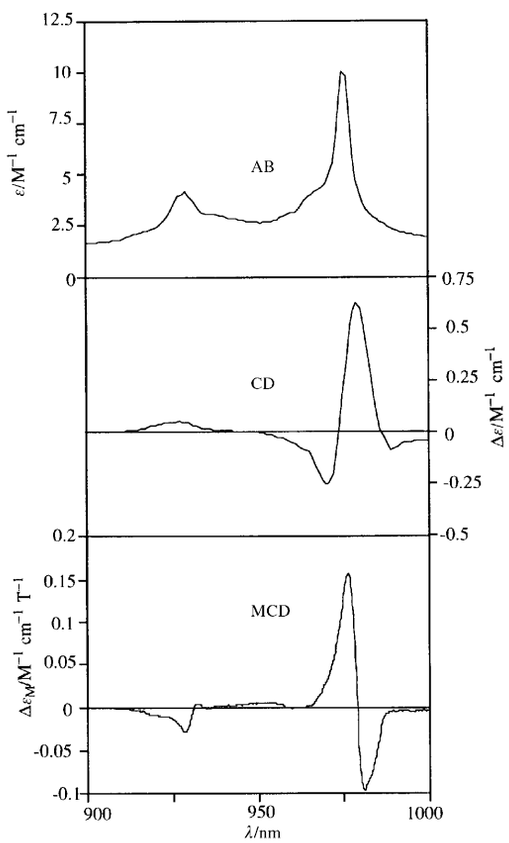

Fig. 4 NIR absorption (top), NIR CD of the (Λ–Δ)-$Cr(acac)_2(ox)$-$Yb(HBpz_3)_2$ complex (middle) and NIR MCD of the $Cr(acac)_2(ox)Yb$-$(HBpz_3)_2$ complex (bottom) in CH_2Cl_2.

a negative, positive and negative CD peak from the longer wavelength side, whereas the latter group gives a positive and a negative MCD and a positive CD as shown in Fig. 4. These multiple MCD and CD components arise from the ligand field splitting within the $^2F_{7/2} \rightarrow {}^2F_{5/2}$ transitions of the Yb(III) chromophore. There are expected to be a few transitions from four Kramers doublets of the ground $^2F_{7/2}$ state to three of the excited $^2F_{5/2}$ states, as schematically shown in Fig. 5. This CD pattern is similar to that recently reported[10] but the number of CD components is somewhat different. A similar CD pattern with much weaker intensity is observed for **3**, a diastereomeric mixture of Λ- and Δ-[Yb(HBpz$_3$)$_2$(*S*-pba)], though the shortest wavelength component (1–3′) could not be observed owing to the weak CD intensity as shown in Fig. 6.

The corresponding MCD components of the racemic *RS*-pba complex **4** are very similar in position, pattern and intensity to those of the racemic Cr–Yb complex as compared in Figs. 4 and 6. This fact suggests that **4** and Cr(ox)Yb have similar electronic states and that there seems to be too little Cr–Yb intramolecular magnetic interaction to be detected by MCD at room temperature. The CD spectra of both the

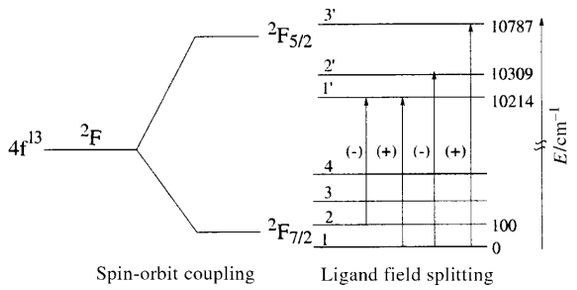

Fig. 5 Energy level diagram for Yb(III) complexes: the figures on the right hand side (cm^{-1}) are tentatively assigned to each transition energy from two of the four ground Kramers doublets to the three excited states and (−) and (+) from left to right refer to the CD signs from the lower frequency side.

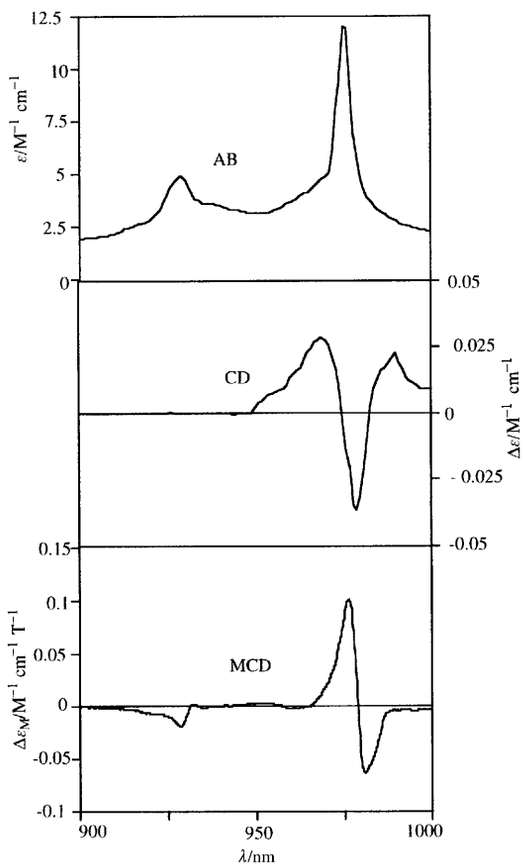

Fig. 6 NIR absorption (AB) (top), NIR CD of a diastereomeric mixture **3** of Δ-[Yb(HBpz$_3$)$_2$(*S*-pba)] and Λ-[Yb(HBpz$_3$)$_2$(*S*-pba)] (middle) and NIR MCD of [Yb(HBpz$_3$)$_2$(*RS*-pba)] (**4**) (bottom) in CH_2Cl_2.

Yb complexes are found to exhibit higher resolution than the corresponding MCD spectra as shown in Figs. 4 and 6; especially as the longest wavelength MCD component (2–1′) is not observed. This is in contrast to the case of Na_3[Eu(III)-(ODA)$_3$]·2$NaClO_4$·6H_2O, where the MCD in the $^7F_0 \rightarrow {}^5D_2$ transition gives more components than the CD spectrum.[28]

On the other hand, the racemic and chiral Dy(**2**) complexes exhibit two groups of MCD and CD components near 914 nm (10940 cm^{-1}) and 813 nm (12300 cm^{-1}) assignable to the $^6H_{15/2} \rightarrow {}^6F_{7/2}$ and $^6H_{15/2} \rightarrow {}^6F_{5/2}$ transitions within the $4f^{19}$ configuration,[29] respectively, from the longer wavelength side as seen in Fig. 7. This is the first observation of the NIR CD for Dy(III) complexes. It is noted that the MCD components of the shorter wavelength component ($^6H_{15/2} \rightarrow {}^6F_{5/2}$) are similar in position, intensity and sign to those of Dy(ClO_4)$_3$ in aqueous solution.[30] The MCD spectrum of the Dy complex is less well

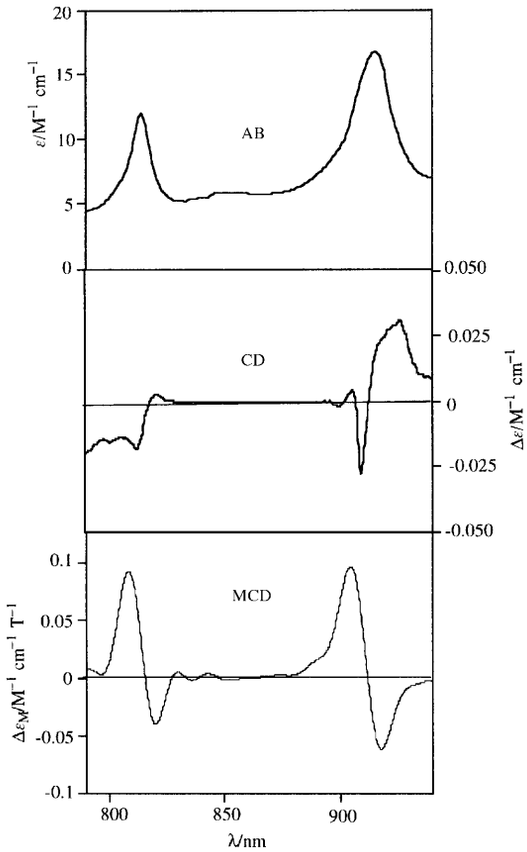

Fig. 7 NIR absorption (AB) (top) and NIR CD (middle) of (Λ–Δ)-[Cr(acac)$_2$(ox)Dy(HBpz$_3$)$_2$] **2** and NIR MCD of the racemic [(acac)$_2$-Cr(ox)Dy(HBpz$_3$)$_2$] (bottom) in CH_2Cl_2.

resolved than the corresponding CD spectrum which demonstrates the multiple components due to the ligand field splitting (Fig. 7) as seen for the Yb complexes. Accordingly the CD spectra are expected to provide more information on stereochemistry and electronic state than the MCD spectra at room temperature. The present solution NIR MCD spectra are the first example, apart from the solid MCD spectra of the Yb(III) ion in $LiNbO_3$ crystals,[31] and the solution MCD spectra in the shorter wavelength $^6H_{15/2} \rightarrow {}^6F_{5/2}$ transition of the Dy(III) perchlorate in aqueous solution.[30]

The degree of chirality is assessed by the dissymmetry factor $g = \Delta\varepsilon_{ext}/\varepsilon_{max}$. There is found to be a large difference in the g values of the Yb complexes; 0.063 for complex **1** and 0.0024 for **3**. This fact demonstrates that the chiral structures in the solid state are mostly retained even in solution. That is, complex **1** gives the configurational CD ($\Delta\varepsilon(\Lambda)$), whereas the optical activity in the 4f→4f transitions of complex **3** could be affected by the following three factors. The first is the vicinal effect ($\Delta\varepsilon$(*S*-pba)) originating from the coordinated *S*-pba ligand, since the CD intensities for each diastereomer of Λ- and Δ-[Yb(HBpz$_3$)$_2$(*S*-pba)] stand for $\Delta\varepsilon(\Lambda) + \Delta\varepsilon$(*S*-pba) and $\Delta\varepsilon(\Delta) + \Delta\varepsilon$(*S*-pba). The summation results in $2\Delta\varepsilon$(*S*-pba), assuming $\Delta\varepsilon(\Lambda) = -\Delta\varepsilon(\Delta)$. The second is a small diastereomeric excess in solution. The third is $\Delta\varepsilon(\Lambda) = -\Delta\varepsilon(\Delta)$, when the crystal structural difference in the diastereomers is rigorously retained in solution. Since the difference in solid structure would result from the crystal packing effect, the third point is unlikely in solution. Thus, the weak CD or the small g values may result from the vicinal effect and/or a small excess of one diastereomer due to the equilibrium displacement.

The CD intensities and g values (≈*ca.* 2×10^{-3}) of the Dy complex, **2**, are much weaker than those of the corresponding Yb complex, **1**. These differences in g values are elucidated by the following consideration. The selection rule for the optical

activity of Ln complexes proposed by Richardson[32] indicates that the $^2F_{7/2}\rightarrow{}^2F_{5/2}$ transition with $\Delta J = 1$, $\Delta S = 0$, $\Delta L = 0$ for Yb complexes is magnetic dipole allowed to the zeroth order and attains an electric dipole strength to the first order in the interconfigurational operator (V_u) which mixes even-parity 5d states into the odd-parity 4f electronic states. However, both the $^6H_{15/2}\rightarrow{}^6F_{5/2}$ and $^6H_{15/2}\rightarrow{}^6F_{7/2}$ transitions with $\Delta J = 4,5$, $\Delta S = 0$, $\Delta L = 2$ for Dy complexes are magnetic and electric dipole forbidden in the zeroth order and are only allowed to the first order in the V_u as well as the intraconfigurational V_g operator leading to the crystal field splitting. According to Richardson's classification,[32] the dissymmetry factor of the former Yb transition is grouped as DII, while the latter Dy transitions belong to the DIII class. Since the *g* values of the DII and DIII are qualitatively dependent on $(V_u)^{-1}$ and (V_g/V_u), respectively, the *g* values of the DII group are larger than those of the DIII group. In fact, the *g* value of complex **2** is *ca.* 2×10^{-3} which is in an order of magnitude smaller than that of DII for the configurational chiral complex **1**. The increasing order of the *g* value (Dy < Yb) is in accordance with that (DIII < DII) predicted by the selection rule. Therefore, the above consideration supports that not only complex **1** but also complex **2** takes the configurational chirality around the Dy(III) entity with the Λ-Cr(ox)–Δ-Dy configurations. The present *g* values establish the criterion for determining the configurational chirality around Yb and Dy ions. It follows that the Δ absolute configuration around the *SAPR*-8-Ln$(HBpz_3)_2$ moiety gives the positive sign for the major CD component at 975 nm (10260 cm^{-1}) for complex **1** and near 914 nm (10940 cm^{-1}) for complex **2**. This criterion for the absolute configuration of *SAPR*-8 complexes may also be applied to the recent result ($(-)_{980}^{\Delta\varepsilon}$ *vs.* Λ) for Yb(DOTMA).[10]

The present NIR CD spectra are the first observations of 4f→4f transitions for the configurational chiral dinuclear 3d–4f assembly with no asymmetric carbon atom, promising versatility in optical activity or CPL in 3d–4f interactions in the novel assembled (Λ–Δ)-Cr(ox)Ln systems.

Conclusion

In view of the solution NIR CD spectra of **1**, it is seen that a pair of Λ-$[Cr(ox)(acac)_2]^-$ and Δ-$[Yb(HBpz_3)_2]^+$ results from the stereospecific assembly, through chiral discrimination around the Yb ion, induced by the absolute configuration of the Cr(III) entity and *not* from accidental pickup from a racemic mixture of Λ-Cr(ox)-Δ-Yb and Λ-Cr(ox)-Λ-Yb diastereomers. The same situation is encountered in the case of the racemate. To our knowledge, this is the first example of the stereospecific (Λ–Δ)-Cr(ox)Ln assembly with configurational chirality of the lanthanide complexes in solution without asymmetric carbon atoms. It is noted that this kind of stereospecific assembly occurs in spite of the fact that the long Cr–Yb distance [5.631 Å (for the racemate) and 5.672 Å (for **1**)] is very similar to that found in the isolated *rac*- and *meso*-$[Ru_2(\mu\text{-bpym})(bpy)_4]^{4+}$ (bpym = bipyrimidine)[33] and much longer than that for *rac*- and *meso*-$[Cr_2(OH)_2(rac\text{-chxn})_4]^{4+}$ (chxn = 1,2-*trans*-cyclohexanediamine).[34] In fact, the space-filling molecular model indicates that the Cr(ox)Yb complex has more space between the ligands ($acac^-$ and $BHpz_3^-$) than in the Ru complexes.[33] In addition, the chiral (Λ–Δ)-Cr(ox)Ln complexes were found to remain unchanged in dichloromethane even after standing for a few months. Such robustness toward racemization around the labile Ln ions in solution may be associated with a long range nonbonding intramolecular interaction between the coordinated $HBpz_3^-$ and $acac^-$ as well as the unexpected rigid solution behavior, as claimed for $[Yb(HBpz_3)_3]$ from NMR studies.[15] Further study is required to determine what governs long distance chiral discrimination or the configurational chirality around the Ln(III) ions on assembly with the optically active Cr(III) complex as well as what factors result in robustness towards racemization.

Acknowledgements

We gratefully acknowledge support of this research by a Grant-in-Aid for Scientific Research (No. 10304056) from the Ministry of Education, Science and Culture.

References

1 J. P. Riehl and F. S. Richardson, *Chem. Rev.*, 1986, **86**, 1.
2 C. Piguet and J.-C. G. Bünzli, *Chem. Soc. Rev.*, 1999, **28**, 347.
3 S. Misumi, S. Kida and T. S. Isobe, *Spectrochim. Acta*, 1968, **24A**, 271.
4 L. I. Katzin, *Inorg. Chem.*, 1968, **7**, 1138; L. I. Katzin, *Inorg. Chem.*, 1969, **8**, 1649.
5 R. Prados, L. G. Stadtherr, Jr., H. Donato and R. B. Martin, *J. Inorg. Nucl. Chem.*, 1974, **36**, 689.
6 (*a*) H. G. Brittain and F. S. Richardson, *J. Am. Chem. Soc.*, 1977, **99**, 65; (*b*) P. Biscarini, *Inorg. Chim. Acta*, 1983, **74**, 65; (*c*) N. Coruh, G. L. Hilmes and J. P. Riehl, *Inorg. Chem.*, 1988, **27**, 3647; (*d*) R. S. Dickens, J. A. K. Howard, C. W. Lehman, J. Moloney, D. Parker and R. D. Peacock, *Angew. Chem., Int. Ed. Engl.*, 1997, **36**, 521; (*e*) H. G. Brittain, *Coord. Chem. Rev.*, 1998, **48**, 243; (*f*) R. S. Dickens, J. A. K. Howard, C. L. Maupin, J. Moloney, D. Parker, R. D. Peacock, J. P. Riehl and G. Siligardi, *New J. Chem.*, 1998, **22**, 891.
7 B. Norden and I. Grenthe, *Acta Chem. Scand.*, 1972, **26**, 407.
8 R. W. Schwartz, A. Banerjee, A. C. Sen and M. Chowdhury, *J. Chem. Soc., Faraday Trans. II*, 1980, **76**, 620.
9 D. Parker and J. A. G. Williams, *J. Chem. Soc., Dalton Trans.*, 1996, 3613.
10 (*a*) L. D. Bari, G. Pintacuda and P. Salvadori, *J. Am. Chem. Soc.*, 2000, **122**, 5557; (*b*) L. D. Bari, G. Pintacuda, P. Salvadori, R. S. Dickens and and D. Parker, *J. Am. Chem. Soc.*, 2000, **122**, 9257.
11 C. L. Maupin, D. Parker, J. A. G. Williams and J. P. Riehl, *J. Am. Chem. Soc.*, 1998, **120**, 10563.
12 R. S. Dickins, J. A. K. Howard, C. L. Maupin, J. M. Moloney, D. Parker, J. P. Riehl, G. Siligardi and J. A. G. Williams, *Chem. Eur. J.*, 1999, **5**, 1095.
13 A. Beeby, R. S. Dickins, S. FitzGerald, L. J. Govenlock, C. L. Maupin, D. Parker, J. P. Riehl, G. Siligardi and J. A. G. Williams, *Chem. Commun.*, 2000, 1183.
14 (*a*) A. F. Cockerill, G. L. O. Davies, R. C. Harden and D. M. Rackham, *Chem. Rev.*, 1973, **73**, 553; (*b*) J. Ren, C. S. Springer, Jr. and A. D. Sherry, *Inorg. Chem.*, 1997, **36**, 3493.
15 M. V. R. Stainer and J. Takats, *J. Am. Chem. Soc.*, 1983, **105**, 410.
16 T. Sanada, T. Suzuki and S. Kaizaki, *J. Chem. Soc., Dalton Trans.*, 1998, 959.
17 T. Sanada, T. Suzuki, T. Yoshida and S. Kaizaki, *Inorg. Chem.*, 1998, **37**, 4712.
18 S. Trofimenko, *J. Chem. Soc.*, 1967, **89**, 3170.
19 F. P. Dwyer, I. K. Reid and A. M. Sargeson, *Aust. J. Chem.*, 1965, **18**, 1919.
20 M. A. J. Moss and C. J. Jones, *J. Chem. Soc., Dalton Trans.*, 1990, 581.
21 A. C. T. North, D. C. Phillips and F. S. Mathews, *Acta Crystallogr., Sect. A*, 1968, **24**, 351.
22 P. Choppens, L. Leiserowitz and D. Rabinovich, *Acta Crystallogr.*, 1965, **18**, 1035.
23 G. M. Sheldrick, *Acta Crystallogr., Sect. A*, 1990, **46**, 467.
24 Molecular Structure Corporation and Rigaku Co. Ltd., TeXsan, Single Crystal Structure Analysis Software, version 1.9, 1998, MSC, The Woodlands, TX 77381-5209, USA and Rigaku Co. Ltd., Akishima, Tokyo 196-8666, Japan.
25 H. D. Flack, *Acta Crystallogr., Sect. A*, 1983, **39**, 876.
26 S. Kaizaki, J. Hidaka and Y. Shimura, *Inorg. Chem.*, 1973, **12**, 135.
27 (*a*) R. Kuroda and S. F. Mason, *J. Chem. Soc., Dalton Trans.*, 1979, 273; (*b*) R. D. Peacock, *J. Chem. Soc., Dalton Trans.*, 1983, 291.
28 W. T. Carnall, P. R. Fields and K. Rajnak, *J. Chem. Phys.*, 1968, **49**, 4424.
29 C. Gorller-Walrand, P. Verhoeven, J. D'Olieslager, L. Fluyt and K. Binnemanns, *J. Chem. Phys.*, 1994, **100**, 815.
30 C. Gorller-Walrand, H. Peeters, Y. Beyens, N. D. Moitie-Neyt and M. Behets, *Nouv. J. Chim.*, 1980, **4**, 715.
31 C. Bonardi, R. A. Carvalho, H. C. Basso, M. C. Terrile, G. K. Cruz, L. E. Bausa and J. Garcia Sole, *J. Chem. Phys.*, 1999, **111**, 6042.
32 F. S. Richardson, *Inorg. Chem.*, 1980, **19**, 2806.
33 X. Hua and A. von Zelewsky, *Inorg. Chem.*, 1995, **34**, 5791.
34 S. Kaizaki, N. Azuma and A. Fuyuhiro, *Inorg. Chim. Acta*, 1998, **274**, 210.
35 C. K. Johnson, ORTEP II, Report ORNL-5138, Oak Ridge National Laboratory, Oak Ridge, TN, 1976.